International Journal of Physical Sciences Vol. 6(36), pp. 8018-8026, 30 December, 2011
Available online at http://www.academicjournals.org/IJPS
DOI: 10.5897/IJPS11.1425
ISSN 1992 - 1950 ©2011 Academic Journals

Full Length Research Paper

Study of slip and induced magnetic field on the peristaltic flow of pseudoplastic fluid

S. Noreen[1], T. Hayat[2,3]* and A. Alsaedi[3]

[1]Department of Mathematics, Comsats Institute of Information Technology, Attock 43600, Pakistan.
[2]Department of Mathematics, Quaid-I-Azam University 45320, Islamabad 44000, Pakistan.
[3]Department of Mathematics, Faculty of Science, King Abdul Aziz University, P. O. Box 80203, Jeddah 21589, Saudi Arabia.

Accepted 28 September, 2011

Effects of slip and induced magnetic field on the peristaltic flow of pseudoplastic fluid have been investigated. The corresponding shear stress is employed in defining the slip condition. The fluid is considered in a channel with non-conducting walls. The arising flow problem is solved in view of the assumptions of long wavelength and low Reynolds number. The stream function, pressure gradient and magnetic force function are computed. Pumping phenomenon is analyzed. Variations of pertinent involved parameters on the flow quantities of interest are described.

Key words: Induced magnetic field, slip condition, pseudoplastic fluid.

INTRODUCTION

The study of peristaltic flows is important in several processes of engineering and physiology, such as swallowing of food through the esophagus, chyme movement in the gastrointestinal tract, in the ductus efferentes of the male reproductive system, sanitary fluid transport, urine transport from kidney to bladder, lymph transport in the lymphatic vessels, in vasomotion of small blood vessels, in cell separators, arthropumps, finger and roller pumps and heart lung machine. No doubt, much effort has been devoted to the analysis of peristaltic flows under diverse aspects since the earliest research (Latham, 1966; Shapiro et al., 1969). Sapna (2009) discussed the influence of stenosis on the flow resistance, apparent viscosity and wall shear stress in an artery. He treated blood as the power law and Casson fluids. Analytic solution for two-dimensional flow of blood with variable viscosity and magnetic field is developed (Singh and Rathee, 2010). Singh and Rathee (2011) also studied the non-Newtonian effects on the blood flow through stenosed vessel in the presence of magnetic field and porous space. Few latest developments on the peristalsis may be mentioned in the recent investigations (Vajravelu et al., 2011; Tripathi et al., 2010, 2011; Elmaboud and Mekheimer, 2011; Hayat et al., 2008; Hayat and Noreen, 2010; Hayat and Hina, 2010; Nadeem and Akram, 2010).

It is however noticed that limited attention is paid to the peristaltic flows of non-Newtonian fluids when no-slip condition is not adequate. Ebaid (2008) reported the effects of wall slip and induced magnetic field on the peristaltic flow of viscous fluid in an asymmetric channel. Effects of slip condition and wall properties on the magnetohydrodynamic (MHD) peristaltic transport of viscous fluid have been examined (Srinivas et al., 2009). They presented the flow analysis with heat transfer. Shehawy et al. (2006) studied the peristaltic flow of a Maxwell fluid with slip effect. The peristaltic flow of couple stress fluid in uniform and non-uniform channel subject to slip condition has been investigated (Sobh, 2008). Hayat et al. (2008) have discussed the influence of partial slip on the peristaltic flow in a porous medium. Ali et al. (2008) addressed the problem of MHD peristaltic transport of variable viscosity Newtonian fluid in a channel with slip effect. The simultaneous effects of partial slip and heat transfer on the peristaltic flow of viscous fluid in a two-dimensional channel are reported (Hayat et al., 2010). In continuation, Hayat et al. (2008) analyzed the features of slip on the peristaltic motion of third order fluid in an asymmetric channel. On the other hand, the effect of an induced magnetic field on peristaltic

*Corresponding author. E-mail: pensy_t@yahoo.com.

motion in a channel is yet to be addressed properly. Vishnyakov and Pavlov (1972) conducted first such study for a viscous fluid. Mekheimer (2008) has analyzed the MHD flow of conducting couple stress fluid in a symmetric channel. Nadeem and Akram (2011) extended the research of Mekheimer (2008) for asymmetric channel. Hayat et al. (2010) studied the induced magnetic field variation on the peristaltic mechanism of incompressible third order fluid in a symmetric channel. In another investigation Hayat et al. (2011) studied the slip and induced magnetic field effects on peristaltic motion of Phan-Thien-Tanner (PTT) fluid. Shit et al. (2010) dealt with the peristaltic flow analysis of an incompressible magneto-micropolar fluid in an asymmetric channel in the presence of an induced magnetic field.

The present research has been undertaken to discuss the simultaneous effects of slip and induced magnetic field on the peristaltic transport of non-Newtonian fluid in a channel. The constitutive equations of pseudoplastic fluid have been employed in the mathematical formulation. The features of various interesting parameters are analyzed through graphs. This paper is organized as follows: Subsequently, the study deals with the problem formulation, after which it presented expressions for small viscoelastic parameter ξ . This is followed by discussion, regarding the pumping phenomenon and other flow quantities of interest.

FORMULATION

We investigate magnetohydrodynamic (MHD) pseudoplastic fluid in a planar channel of uniform thickness 2a. Let a sinusoidal wave propagates with the speed c along the non-conducting channel walls. The stream wise coordinates is taken as $\overline{X}$ and that normal to it is denoted by $\overline{Y}$. A constant magnetic field $(\text{with strength } H_0)$ is exerted in transverse direction. This results in an induced magnetic field $\mathbf{H}\left(\overline{h}_{\overline{x}}\left(\overline{X},\overline{Y},\overline{t}\right),\overline{h}_{\overline{y}}\left(\overline{X},\overline{Y},\overline{t}\right),0\right)$. The total magnetic field thus, is $\mathbf{H}^{+}\left(\overline{h}_{\overline{x}}\left(\overline{X},\overline{Y},\overline{t}\right),H_0+\overline{h}_{\overline{y}}\left(\overline{X},\overline{Y},\overline{t}\right),0\right)$. The wave shape for the present study is considered as follows:

$$\overline{h}(\overline{X},\overline{t})=a+b\sin\left(\frac{2\pi}{\lambda}\left(\overline{X}-c\overline{t}\right)\right), \tag{1}$$

where λ is the wavelength, a is the channel half width, $\overline{t}$ is the time and b is the wave amplitude. The velocity $\mathbf{V}$ in fixed frame $\left(\overline{X},\overline{Y}\right)$ is defined by:

$$\mathbf{V}=[\overline{U}(\overline{X},\overline{Y},\overline{t}),\overline{V}(\overline{X},\overline{Y},\overline{t}),0], \tag{2}$$

in which $\overline{U}$ and $\overline{V}$ denote the velocity components parallel to the $\overline{X}$ and $\overline{Y}-$ axes, respectively. The governing equations for the considered problem are

$$\nabla\cdot\mathbf{V}=0, \tag{3}$$

$$\begin{aligned}\rho\frac{d\mathbf{V}}{dt}&=\operatorname{div}\mathbf{T}+\mu_e\left(\nabla\times\mathbf{H}^{+}\right)\times\mathbf{H}^{+}\\&=\operatorname{div}\mathbf{T}+\mu_e\left[\left(\mathbf{H}^{+}\cdot\nabla\right)\mathbf{H}^{+}-\frac{\nabla\mathbf{H}^{+^2}}{2}\right],\end{aligned} \tag{4}$$

$$\frac{\partial\mathrm{H}^{+}}{\partial t}=\nabla\times\left(V\times H^{+}\right)+\frac{1}{\varepsilon}\nabla^2H^{+} \tag{5}$$

In the foregoing expressions $\varsigma=\sigma\mu_e$ is the magnetic diffusivity, σ is the electrical conductivity, μ_e is the magnetic permeability, ρ is density, d/dt is the material derivative and $\mathbf{T}$ is the Cauchy stress tensor. Further, the Maxwell's equations (with no displacement current) can be put into the following arrangement.

$$\nabla\cdot\mathbf{E}=0,\qquad \nabla\cdot\mathbf{H}=0, \tag{6}$$

$$\nabla\times\mathrm{E}=-\mu_e\frac{\partial\mathrm{H}}{\partial t},\nabla\times\mathrm{H}=J_9 \tag{7}$$

$$J=\sigma\left(\mathrm{E}+\mu_e\left(V\times\mathrm{H}\right)\right)_7 \tag{8}$$

where $\mathbf{J},\mathbf{E}$ and $\mathbf{H}$ respectively denote the current density, the electric field and the magnetic field, respectively. The expression for $\overline{\mathbf{T}}$ is $[25]$. (Boger, 1977).

$$\overline{\mathbf{T}}=-\overline{P}\mathbf{I}+\overline{\mathbf{S}}, \tag{9}$$

$$\overline{\mathbf{S}}+\overline{\lambda}_1\overline{\mathbf{S}}^{\nabla}+\frac{1}{2}\left(\overline{\lambda}_1-\overline{\mu}_1\right)\left(\overline{\mathbf{A}}_1\overline{\mathbf{S}}+\overline{\mathbf{S}}\,\overline{\mathbf{A}}_1\right)=\mu\overline{\mathbf{A}}_1, \tag{10}$$

$$\overline{\mathbf{S}}^{\nabla}=\frac{d\overline{\mathbf{S}}}{dt}-\overline{\mathbf{S}}\overline{\mathbf{L}}^{T}-\overline{\mathbf{L}}\overline{\mathbf{S}}, \tag{11}$$

$$\overline{\mathbf{A}}_1=\overline{\mathbf{L}}+\overline{\mathbf{L}}^{\mathbf{T}},\qquad \overline{\mathbf{L}}=\operatorname{grad}\overline{\mathbf{V}}, \tag{12}$$

where $\overline{\mathbf{I}}$, $\overline{P}$, $\overline{\mathbf{S}}$, $\overline{\mathbf{A}}_1$ μ, $\overline{\mathbf{S}}^{\nabla}$ and $\overline{\mu}_1$ and $\overline{\lambda}_1$, respectively indicate the identity tensor, the pressure, the extra stress tensor, the first Rivlin-Ericksen tensor, the dynamic viscosity, the upper-convected derivative and the relaxation times. The transformations for the coordinates, pressure and velocity components in wave frame are introduced as follows:

$$\begin{aligned} &\bar{x}=\bar{X}-c\bar{t}, \qquad \bar{y}=\bar{Y}, \quad \bar{p}(\bar{x},\bar{y})=\bar{P}(\bar{X},\bar{Y},\bar{t}) \\ &\bar{u}(\bar{x},\bar{y})=\bar{U}-c, \qquad \bar{v}(\bar{x},\bar{y})=\bar{V}, \end{aligned} \tag{13}$$

The aforementioned fundamental equations give:

$$\frac{\partial \bar{u}}{\partial \bar{x}}+\frac{\partial \bar{v}}{\partial \bar{y}}=0, \tag{14}$$

$$\rho\left(\bar{u}\frac{\partial}{\partial \bar{x}}+\bar{v}\frac{\partial}{\partial \bar{y}}\right)\bar{u}+\frac{\partial \bar{p}}{\partial \bar{x}}=\frac{\partial \bar{S}_{xx}}{\partial \bar{x}}+\frac{\partial \bar{S}_{xy}}{\partial \bar{y}}-\frac{\mu_e}{2}\left(\frac{\partial H^{+^2}}{\partial \bar{x}}\right)+\mu_e\left(\bar{h}_{\bar{x}}\frac{\partial \bar{h}_{\bar{x}}}{\partial \bar{x}}+\bar{h}_{\bar{y}}\frac{\partial \bar{h}_{\bar{x}}}{\partial \bar{y}}+H_0\frac{\partial \bar{h}_{\bar{x}}}{\partial \bar{y}}\right), \tag{15}$$

$$\rho\left(\bar{u}\frac{\partial}{\partial \bar{x}}+\bar{v}\frac{\partial}{\partial \bar{y}}\right)\bar{v}+\frac{\partial \bar{p}}{\partial \bar{y}}=\frac{\partial \bar{S}_{yx}}{\partial \bar{x}}+\frac{\partial \bar{S}_{yy}}{\partial \bar{y}}-\frac{\mu_e}{2}\left(\frac{\partial H^{+^2}}{\partial \bar{y}}\right)+\mu_e\left(\bar{h}_{\bar{x}}\frac{\partial \bar{h}_{\bar{y}}}{\partial \bar{x}}+\bar{h}_{\bar{y}}\frac{\partial \bar{h}_{\bar{y}}}{\partial \bar{y}}+H_0\frac{\partial \bar{h}_{\bar{y}}}{\partial \bar{y}}\right), \tag{16}$$

$$\begin{aligned} 2\mu\frac{\partial \bar{u}}{\partial \bar{x}}=\bar{S}_{xx}+\bar{\lambda}_1\left(\bar{u}\frac{\partial \bar{S}_{xx}}{\partial \bar{x}}+\bar{v}\frac{\partial \bar{S}_{xx}}{\partial \bar{y}}-2\frac{\partial \bar{u}}{\partial \bar{x}}\bar{S}_{xx}-2\frac{\partial \bar{u}}{\partial \bar{y}}\bar{S}_{xy}\right) \\ +\frac{1}{2}\left(\bar{\lambda}_1-\bar{\mu}_1\right)\left(4\bar{S}_{xx}\frac{\partial \bar{u}}{\partial \bar{x}}+2\bar{S}_{xy}\left(\frac{\partial u}{\partial y}+\frac{\partial v}{\partial x}\right)\right), \end{aligned} \tag{17}$$

$$\begin{aligned} 2\mu\frac{\partial \bar{v}}{\partial \bar{y}}=\bar{S}_{yy}+\bar{\lambda}_1\left(\bar{u}\frac{\partial \bar{S}_{yy}}{\partial \bar{x}}+\bar{v}\frac{\partial \bar{S}_{yy}}{\partial \bar{y}}-2\frac{\partial \bar{v}}{\partial \bar{y}}\bar{S}_{yy}-2\frac{\partial \bar{v}}{\partial \bar{x}}\bar{S}_{xy}\right) \\ +\frac{1}{2}\left(\bar{\lambda}_1-\bar{\mu}_1\right)\left(4\bar{S}_{yy}\frac{\partial \bar{v}}{\partial \bar{y}}+2\bar{S}_{xy}\left(\frac{\partial u}{\partial y}+\frac{\partial v}{\partial x}\right)\right), \end{aligned} \tag{18}$$

$$\begin{aligned} \mu\left(\frac{\partial \bar{u}}{\partial \bar{y}}+\frac{\partial \bar{v}}{\partial \bar{x}}\right)=\bar{S}_{xy}+\bar{\lambda}_1\left(\bar{u}\frac{\partial \bar{S}_{xy}}{\partial \bar{x}}+\bar{v}\frac{\partial \bar{S}_{xy}}{\partial \bar{y}}+\frac{\partial \bar{v}}{\partial \bar{x}}\bar{S}_{xx}-\frac{\partial \bar{u}}{\partial \bar{y}}\bar{S}_{yy}\right) \\ +\frac{1}{2}\left(\bar{\lambda}_1-\bar{\mu}_1\right)\left(\left(\bar{S}_{xx}+\bar{S}_{xy}\right)\left(\frac{\partial \bar{u}}{\partial \bar{y}}+\frac{\partial \bar{v}}{\partial \bar{x}}\right)\right), \end{aligned} \tag{19}$$

The dimensionless forms of aforementioned equations in terms of stream function Ψ and magnetic force ϕ function are:

$$\begin{aligned} \mathrm{Re}\delta\left(\frac{\partial \Psi}{\partial y}\frac{\partial}{\partial x}-\frac{\partial \Psi}{\partial x}\frac{\partial}{\partial y}\right)\frac{\partial \Psi}{\partial y}+\frac{\partial p_m}{\partial x}=\delta\frac{\partial S_{xx}}{\partial x}+\frac{\partial S_{xy}}{\partial y}+\delta\mathrm{Re}S^2\left(\frac{\partial \phi}{\partial y}\frac{\partial}{\partial x}-\frac{\partial \phi}{\partial x}\frac{\partial}{\partial y}\right)\frac{\partial \phi}{\partial y} \\ +\mathrm{Re}S^2\frac{\partial^2 \phi}{\partial y^2}, \end{aligned} \tag{20}$$

$$\begin{aligned} -\mathrm{Re}\delta^2\left(\frac{\partial \Psi}{\partial y}\frac{\partial}{\partial x}-\frac{\partial \Psi}{\partial x}\frac{\partial}{\partial y}\right)\frac{\partial \Psi}{\partial x}+\frac{\partial p_m}{\partial y} \\ =\delta\left(\delta\frac{\partial S_{yx}}{\partial x}+\frac{\partial S_{yy}}{\partial y}\right)-\delta^3\mathrm{Re}S^2\left(\frac{\partial \phi}{\partial y}\frac{\partial}{\partial x}-\frac{\partial \phi}{\partial x}\frac{\partial}{\partial y}\right)\frac{\partial \phi}{\partial x}-\mathrm{Re}\delta^2S^2\frac{\partial^2 \phi}{\partial x\partial y}, \end{aligned} \tag{21}$$

$$E=\frac{\partial \Psi}{\partial y}-\delta\left(\frac{\partial \Psi}{\partial y}\frac{\partial \phi}{\partial x}-\frac{\partial \Psi}{\partial x}\frac{\partial \phi}{\partial y}\right)+\frac{1}{R_m}\left(\delta^2\frac{\partial^2}{\partial x^2}+\frac{\partial^2}{\partial y^2}\right)\phi, \tag{22}$$

$$\begin{aligned} 2\delta\frac{\partial^2 \Psi}{\partial y\partial x}=S_{xx}+\lambda_1\left[\left(\delta\frac{\partial \Psi}{\partial y}\frac{\partial}{\partial x}+\frac{\partial \Psi}{\partial x}\frac{\partial}{\partial y}\right)S_{xx}-2\left(\delta\frac{\partial^2 \Psi}{\partial x\partial y}S_{xx}+\frac{\partial^2 \Psi}{\partial y^2}S_{xy}\right)\right] \\ +\frac{1}{2}\left(\lambda_1-\mu_1\right)\left(4\delta S_{xx}\frac{\partial^2 \Psi}{\partial x\partial y}+2S_{xy}\left(\frac{\partial^2 \Psi}{\partial y^2}-\delta^2\frac{\partial^2 \Psi}{\partial x^2}\right)\right), \end{aligned} \tag{23}$$

$$\begin{aligned} -2\delta\frac{\partial^2 \Psi}{\partial y\partial x}=S_{yy}+\lambda_1\left[\delta\left(\frac{\partial \Psi}{\partial y}\frac{\partial}{\partial x}-\frac{\partial \Psi}{\partial x}\frac{\partial}{\partial y}\right)S_{yy}+2\delta\left(\delta\frac{\partial^2 \Psi}{\partial x^2}S_{xy}+\frac{\partial^2 \Psi}{\partial x\partial y}S_{yy}\right)\right] \\ +\frac{1}{2}\left(\lambda_1-\mu_1\right)\left[2S_{xy}\left(\frac{\partial^2 \Psi}{\partial y^2}-\delta^2\frac{\partial^2 \Psi}{\partial x^2}\right)-4\delta S_{yy}\frac{\partial^2 \Psi}{\partial x\partial y}\right], \end{aligned} \tag{24}$$

$$\begin{aligned} \frac{\partial^2 \Psi}{\partial y^2}-\delta^2\frac{\partial^2 \Psi}{\partial x^2}=S_{xy}+\lambda_1\left[\delta\left(\frac{\partial \Psi}{\partial y}\frac{\partial}{\partial x}-\frac{\partial \Psi}{\partial x}\frac{\partial}{\partial y}\right)S_{xy}-\left(\frac{\partial^2 \Psi}{\partial y^2}S_{yy}-\delta^2\frac{\partial^2 \Psi}{\partial x^2}S_{xx}\right)\right] \\ +\frac{1}{2}\left(\lambda_1-\mu_1\right)\left[\left(S_{xx}+S_{yy}\right)\left(\frac{\partial^2 \Psi}{\partial y^2}-\delta^2\frac{\partial^2 \Psi}{\partial x^2}\right)\right], \end{aligned} \tag{25}$$

where Equation 3 is automatically satisfied and

$$\begin{aligned} &\lambda_1=\frac{\bar{\lambda}_1 c}{a},\ x=\frac{\bar{x}}{\lambda},\ y=\frac{\bar{y}}{a},\ t=\frac{c\bar{t}}{\lambda},\ p=\frac{a^2\bar{p}}{c\lambda\mu},\ M^2=\mathrm{Re}S^2R_m, \\ &\delta=\frac{a}{\lambda},\ \bar{S}_{ij}=\frac{a\bar{S}_{ij}}{\mu c}\ (\text{for } i,j=1,2,3),\ u=\frac{\bar{u}}{c},\ v=\frac{\bar{v}}{c},\ \mu_1=\frac{\bar{\mu}_1 c}{a}, \\ &\mathrm{Re}=\frac{ca\rho}{\mu},\ R_m=\sigma\mu_e ac;\ S=\frac{H_0}{c}\sqrt{\frac{\mu_e}{\rho}},\ \phi=\frac{\bar{\phi}}{H_0 a},\ \mu_1=\frac{\bar{\mu}_1 c}{a}, \\ &\bar{h}_{\bar{x}}=\bar{\phi}_{\bar{y}},\ \bar{h}_{\bar{y}}=-\bar{\phi}_{\bar{x}},\ p_m=p+\frac{1}{2}\mathrm{Re}\delta\frac{\mu_e\left(H^+\right)^2}{\rho c^2},\ E=\frac{-\bar{E}}{cH_0\mu_e},\beta=\frac{\bar{\beta}}{a} \\ &u=\frac{\partial \Psi}{\partial y},v=-\delta\frac{\partial \Psi}{\partial x}, \qquad h_x=\frac{\partial \phi}{\partial y},\ h_y=-\delta\frac{\partial \phi}{\partial x}. \end{aligned} \tag{26}$$

Here δ, Re, R_m, S and M are the wave, Reynolds, magnetic Reynolds, Stommer's and Hartman numbers, respectively; α is the amplitude ratio, p_m is the total pressure (which is sum of ordinary and magnetic pressures), E is the electric field strength, β is the slip parameter, Ψ is the stream function, λ_1 and μ_1 are the non-dimensional relaxation times, ϕ is the magnetic force function and

$$h = \frac{\bar{h}}{a} = 1 + \alpha \sin(2\pi x). \tag{27}$$

Adopting long wavelength and low Reynolds number formulation (Haroun, 2007; Mekheimer, 2008; Srinivas, 2009), we can write:

$$\frac{\partial p}{\partial x} = \frac{\partial S_{xy}}{\partial y} + \mathrm{Re}\, S^2 \frac{\partial^2 \phi}{\partial y^2}, \tag{28}$$

$$E = \frac{\partial \Psi}{\partial y} + \frac{1}{R_m}\frac{\partial^2 \phi}{\partial y^2}, \tag{29}$$

$$S_{xx} = (\lambda_1 + \mu_1)\frac{\partial^2 \Psi}{\partial y^2} S_{xy},\ S_{yy} = (-\lambda_1 + \mu_1) S_{xy} \frac{\partial^2 \Psi}{\partial y^2},\ S_{xy} = \frac{\partial^2 \Psi / \partial y^2}{1 + \xi (\partial^2 \Psi / \partial y^2)^2}, \tag{30}$$

with $\left(\lambda_1^2 - \mu_1^2\right) = \xi$ and $\partial p / \partial y = 0$ indicates that $p \neq p(y)$.

The related dimensionless boundary conditions are:

$$\begin{aligned} &\Psi = 0,\ \frac{\partial^2 \Psi}{\partial y^2} = 0, && \frac{\partial \phi}{\partial y} = 0 && at\ y = 0, \\ &\Psi = F,\ \frac{\partial \Psi}{\partial y} + \beta S_{xy} = -1, && \phi = 0 && at\ y = h, \end{aligned} \tag{31}$$

where the dimensionless time mean flow rate F is the wave frame and is related to the dimensionless time mean flow rate θ in the fixed frame as follows:

$$\theta = F + 1, \qquad F = \int_0^h \frac{\partial \Psi}{\partial y}\, dy. \tag{32}$$

Employing Equations 28 to 30, one obtains:

$$\frac{\partial p}{\partial x} = \frac{\partial}{\partial y}\left[\frac{\partial^2 \Psi}{\partial y^2}\left\{1 - \xi\left(\frac{\partial^2 \Psi}{\partial y^2}\right)^2\right\}\right] + M^2\left(E - \frac{\partial \Psi}{\partial y}\right). \tag{33}$$

Compatibility equation in the considered flow is:

$$\frac{\partial^4 \Psi}{\partial y^4} - \xi \frac{\partial^2}{\partial y^2}\left(\frac{\partial^2 \Psi}{\partial y^2}\right)^3 - M^2 \frac{\partial^2 \Psi}{\partial y^2} = 0. \tag{34}$$

SERIES SOLUTIONS

In order to proceed for the perturbation solution, we expand the flow quantities in the forms presented:

$$S_{xy} = S_{0xy} + S_{1xy} + O(\xi)^2, \tag{35}$$

$$\Psi = \Psi_0 + \xi \Psi_1 + O(\xi)^2, \tag{36}$$

$$F = F_0 + \xi F_1 + O(\xi)^2, \tag{37}$$

$$p = p_0 + \xi p_1 + O(\xi)^2, \tag{38}$$

$$\phi = \phi_0 + \xi \phi_1 + O(\xi)^2. \tag{39}$$

Solving the corresponding problems at zeroth and first orders, one has the following expressions for the stream function Ψ, axial pressure gradient dp/dx and magnetic force function ϕ.

$$\begin{aligned} \psi = {} & B_0 M (2h\beta + F - y + \beta + M^2 y^2 \beta^2)(\cosh(hM) - 2y \sinh(hM)) C_1(y) + \xi \\ & \left[-\frac{B_0^4}{8}(F+h)^3 \beta M^4 (\cosh(3My) - \sinh(3My))(C_2(y) + C_3(y) + C_4(y)) \right], \end{aligned} \tag{40}$$

$$\begin{aligned} \frac{dp}{dx} = {} & 2M^2 (\cosh(Mh) - \sinh(Mh)) C_5(y) \\ & + \xi \left[-\frac{B_0^3}{4}(F+h)^3 \beta M^7 (\cosh(3My) - \sinh(3My)) \times C_6(y) \right], \end{aligned} \tag{41}$$

$$\begin{aligned} \phi = {} & \frac{B_0 R_m}{2M} (\cosh(My) - \sinh(My)) C_7(y) \\ & + \xi \left[\frac{B_0^4}{24}(F+h)^3 \beta M^3 (\cosh(3My) - \sinh(3My))(C_8(y) + C_9(y) + C_{10}(y)) \right], \end{aligned} \tag{42}$$

where the involved functions $C_i(y)$ are obtained through simple algebraic computations. The dimensionless axial induced magnetic field h_x, current density J_z and pressure rise ΔP_λ are given by:

$$h_x = \frac{\partial \phi}{\partial y}, \quad J_z = -\frac{\partial h_x}{\partial y}, \quad \Delta P_\lambda = \int_0^1 \left(\frac{dp}{dx}\right)_{y=0} dx, \tag{43}$$

RESULTS AND DISCUSSION

Here, Figures 1 to 5 describe the influence of wall slip

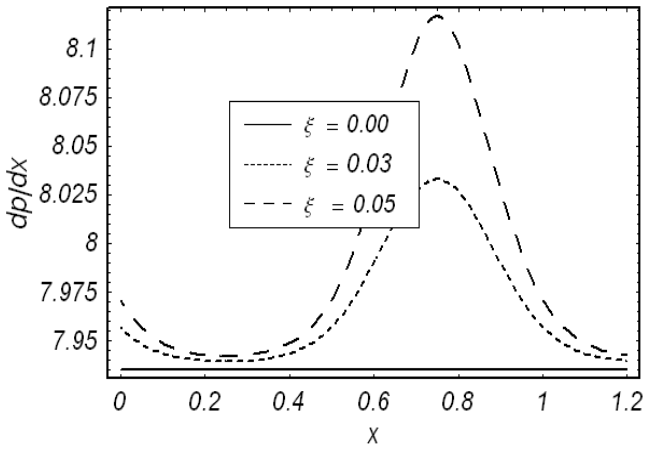

Figure 1a. Pressure gradient dp/dx versus x when $\alpha = 0.2, \beta = 0.02,$ **M** $= 3.3,$ **E** $= 1.5$ **and** $\theta = 1$.

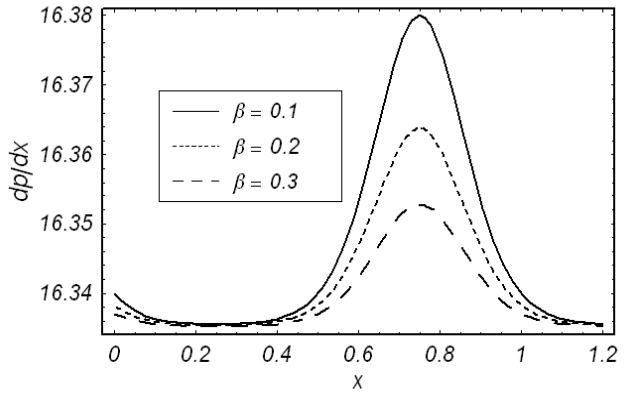

Figure 1b. Pressure gradient dp/dx versus x when $\alpha = 0.2,$ **M** $= 3.3,$ $\xi = 0.02,$ **E** $= 1.6$ **and** $\theta = 1$.

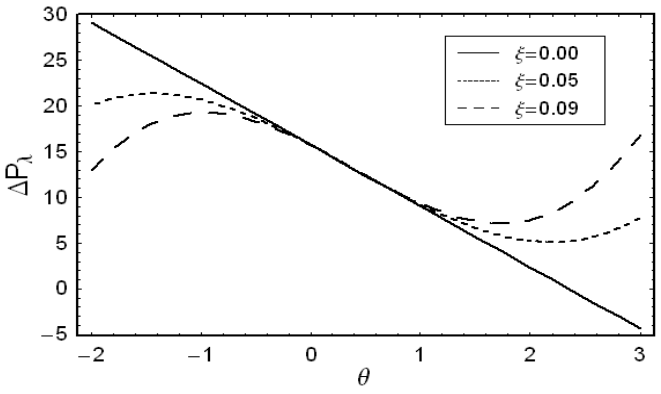

Figure 2a. Pressure gradient dp/dx versus θ when $\alpha = 0.2, \beta = 0.02,$ **x** $= 0.2,$ **M** $= 2.3$ **and** **E** $= 1.5$.

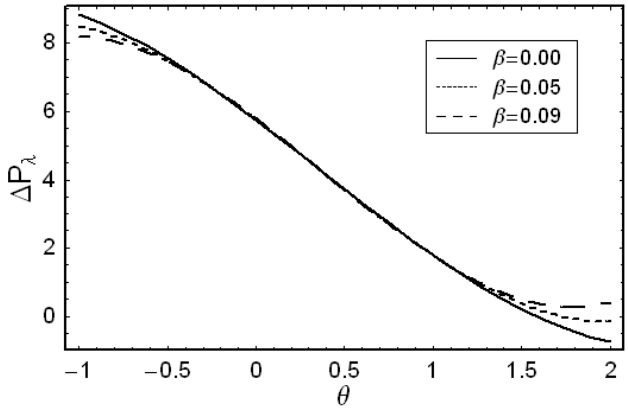

Figure 2b. Pressure gradient dp/dx versus θ when $\alpha = 0.2,$ **M** $= 1.3,$ **x** $= 0.2,$ $\xi = 0.04$ **and** **E** $= 1.5$.

parameter β, relaxation time ξ, Hartman number M, magnetic Reynolds number R_m, the current density J_z, axial induced magnetic field h_x, pressure gradient dp/dx, pressure rise ΔP_λ and velocity distribution u.

Figure 1a illustrates the influence of viscoelastic parameter ξ on the pressure gradient dp/dx. This figure shows that in the wider part of channel $x\varepsilon[0, 0.5]$ and $x\varepsilon[1,1.2]$ the pressure gradient is relatively small. Hence, the flow can easily pass without imposing large pressure gradient. However, in the narrow part of channel $x\varepsilon[0.5,1]$, larger pressure gradient is needed to maintain the same flux to pass through it. It is further observed that the pressure gradient increases by increasing the values of ξ. The magnitude of pressure gradient in viscous fluid is smaller than pseudoplastic fluid. Figure 1b displays the impact of β on axial pressure gradient. It is noticed that magnitude of dp/dx is inversely proportional to β.

The pressure rise against the flow rate is drawn in Figure 2a. This figure depicts that in pumping region $\Delta P_\lambda > 0,$ the pumping rate decreases by increasing ξ. While in the free pumping $\Delta P_\lambda = 0$ and co-pumping region $\Delta P_\lambda < 0$, the pumping rate increases by increasing ξ. Influence of pressure rise ΔP_λ against mean flow rate θ is shown in Figure 2b for different values of β. It is noticed that pressure rise per wavelength is larger in magnitude in case of no-slip condition. It can be seen that the effect of increasing the flow rate is to reduce the pressure rise. Increase in β causes a decrease in the pressure rise. In the pumping

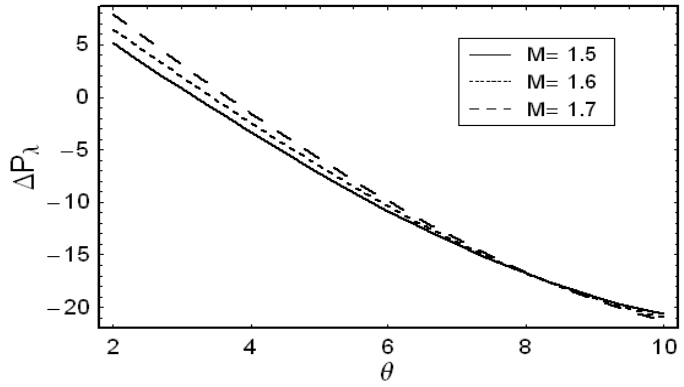

Figure 2c. Pressure rise ΔP_λ versus θ $\alpha = 0.2$, $\beta = 0.02$, $x = -0.2$, $\xi = 0.001$ and $E = 4.5$.

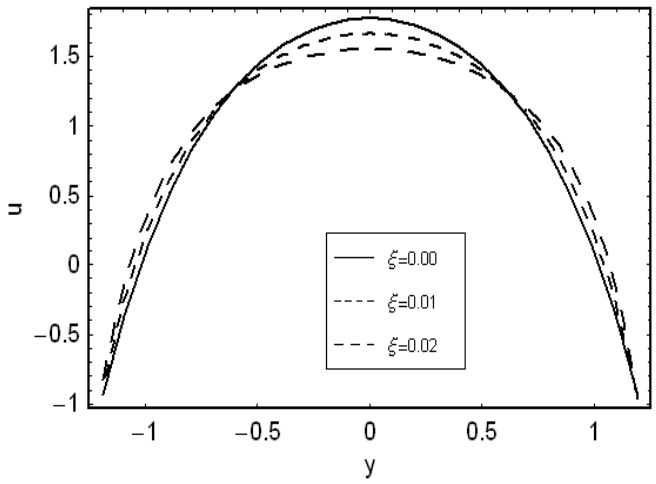

Figure 3a. Axial velocity u for $\beta = 0.01$, $\alpha = 0.2$, $M = 2$, $x = 0.2$ and $\theta = 2.2$.

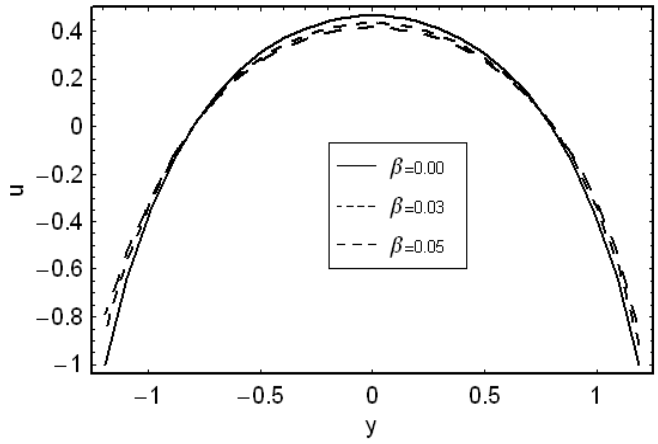

Figure 3b. Axial velocity u for $M = 1.9$, $\alpha = 0.2$, $\xi = 0.03$, $x = 0.2$ and $\theta = 1.1$.

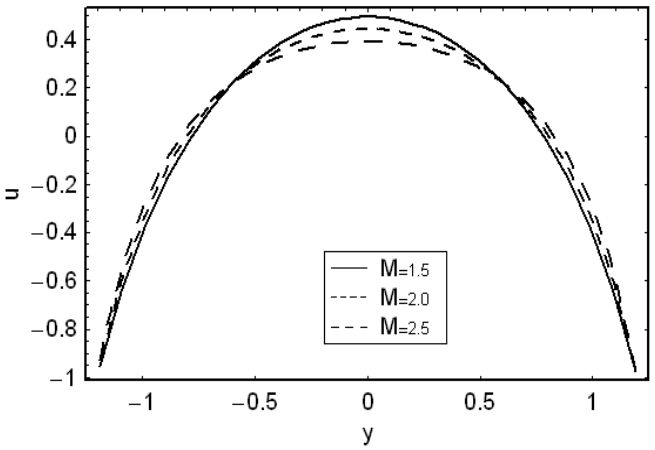

Figure 3c. Axial velocity u for $\beta = 0.01$, $\alpha = 0.2$, $\xi = 0.03$, $x = 0.2$ and $\theta = 1.1$.

($\Delta p_\lambda > 0$) and free pumping ($\Delta p_\lambda = 0$) regions, there is a decrease in pumping rate when β increases. However, augmented pumping rate ($\Delta p_\lambda < 0$) increases by increasing β for the particular values of flow rate. It is also found that the Hartman number M has opposite behavior on pressure rise when compared with the wall slip parameter β (Figure 2c). The variation of M on pressure rise ΔP_λ against mean flow rate θ is plotted in Figure 2c. It is obvious that in the pumping region ($\Delta p_\lambda > 0$), the pumping rate increases by increasing M. The free pumping rate ($\Delta p_\lambda = 0$) increases when M increases. The pumping rate decreases by increasing M in the co-pumping case ($\Delta p_\lambda < 0$) for certain values of flow rate.

Figure 3a to c predicts the influence of ξ, β and M on the longitudinal velocity u. Clearly, the variations of parameters on u at the centre and near the walls of the channel are different. However, at the central line of channel $y = 0$ the largest disparity occurs for ξ and M. Figure 3a and c shows that ξ and M have similar effects on the velocity at the centre of channel. Figure 3b shows that magnitude of velocity increases by increasing β at the upper and lower wall of channel. Increase in wall slip parameter at $y = 0$ has decreasing

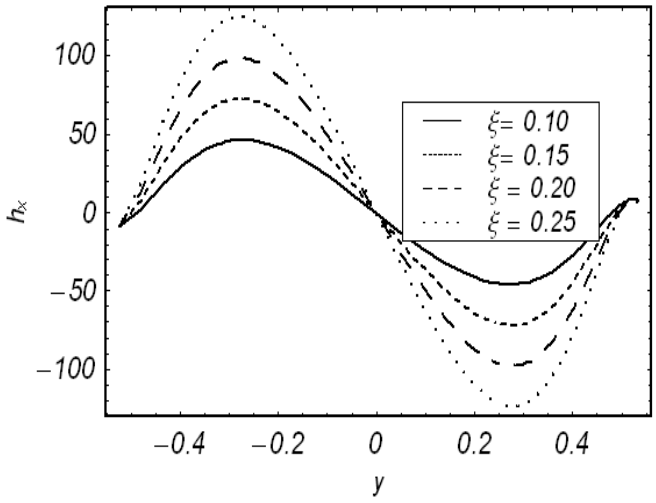

Figure 4a. Axial induced magnetic field h, versus y when $\alpha = 0.5$, $\mathbf{M} = 5.3$, $\mathbf{x} = -0.2$, $\theta = -2.5$, $\mathbf{R}_m = 2$ **and** $\mathbf{E} = 1.5$.

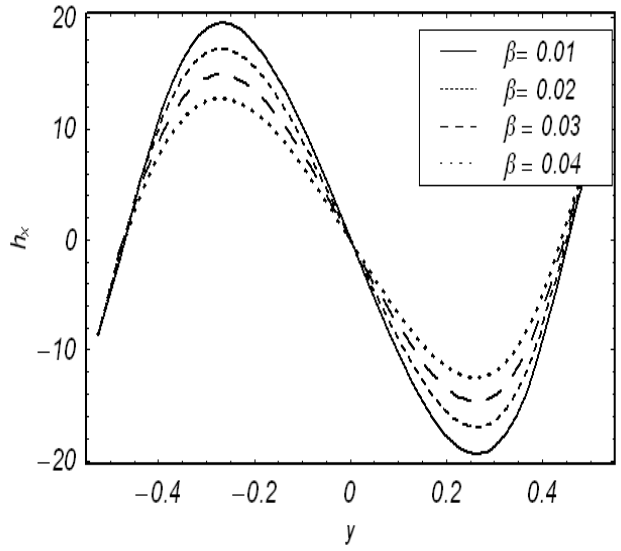

Figure 4b. Axial induced magnetic field h, versus y when $\alpha = 0.5$, $\xi = 0.05$, $\mathbf{x} = -2.5$, $\theta = -2.5$, $\mathbf{R}_m = 2$ **and** $\mathbf{E} = 1.5$.

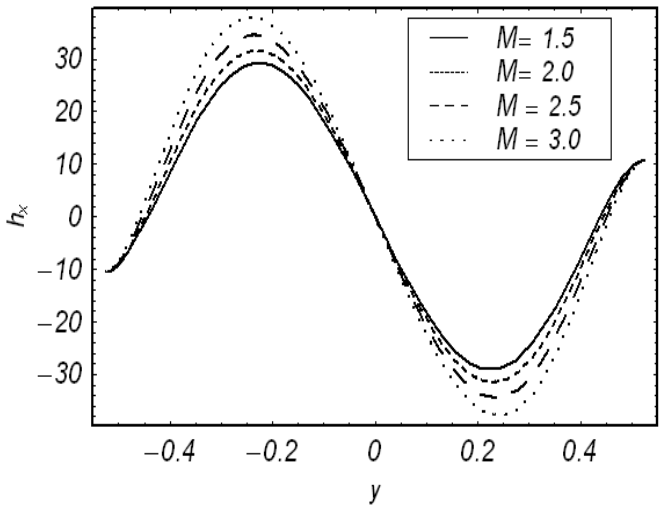

Figure 4c. Axial induced magnetic field h, versus y for $\mathbf{R}_m = 2$, $\alpha = 0.5$, $\xi = 0.05$, $\mathbf{x} = -0.2$, $\theta = 2.5$, $\mathbf{M} = 2.5$ **and** $\mathbf{E} = 1$.

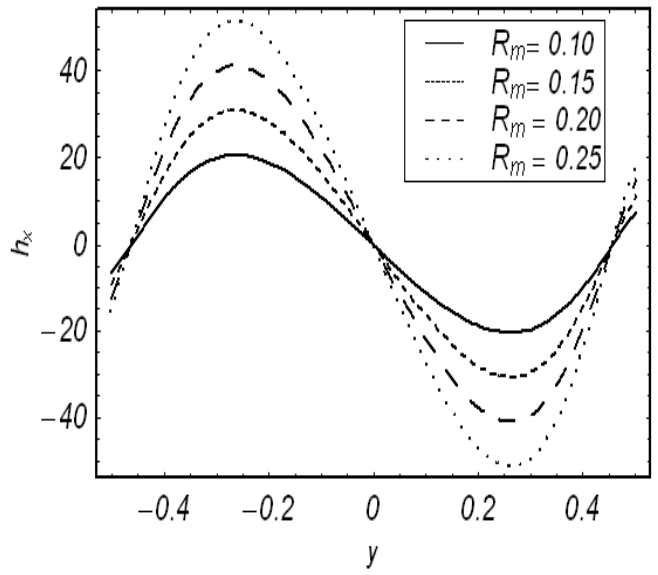

Figure 4d. Axial induced magnetic field h, versus y for $\beta = 0.005, \alpha = 0.2$, $\xi = 0.01$, $\mathbf{x} = -0.2, \theta = -2.5, \mathbf{M} = 5.3$ and $\mathbf{E} = 1.5$.

effect on velocity profile in pseudoplastic fluid.

The magnetic field characteristics have been displayed in Figures 4a to d and 5a to d. Figure 4a, c and d depicts that, the effects of ξ, M and R_m on axial induced magnetic field h_x against y. Here, the magnitude of h_x is a decreasing function of ξ, M and R_m. The induced magnetic field is in one direction in the half region. It is also in the opposite direction in the other half region. The value of h_x is zero when $y = 0$. The effects of slip parameter β on an axial induced magnetic field h_x are illustrated in Figure 4b. The magnitude of h_x is decreasing function of β.

The current density distribution J_z for various values of ξ, β, M and R_m is sketched in Figure 5a to d. We noticed that the curves of J_z are parabolic in nature and the magnitude of the current density J_z increases by increasing the values of ξ, R_m and β. Further, the

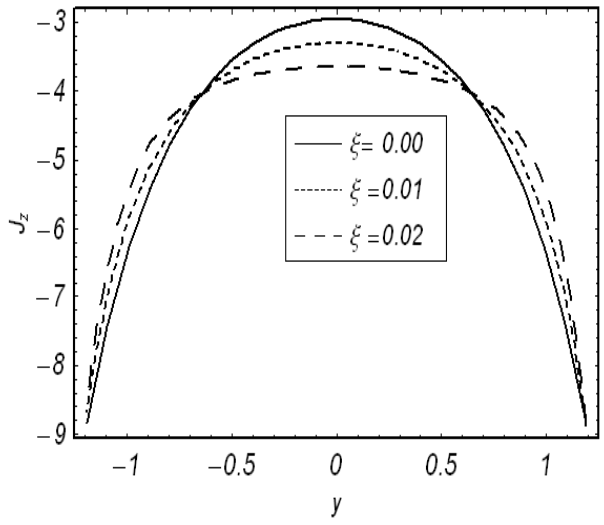

Figure 5a. Current density J_z **versus** y **for** $R_m = 2$, $\beta = 0.01$, $\alpha = 0.2$, $M = 2.5$, $x = 0.2$, $E = 3.5$ **and** $\theta = 2.5$.

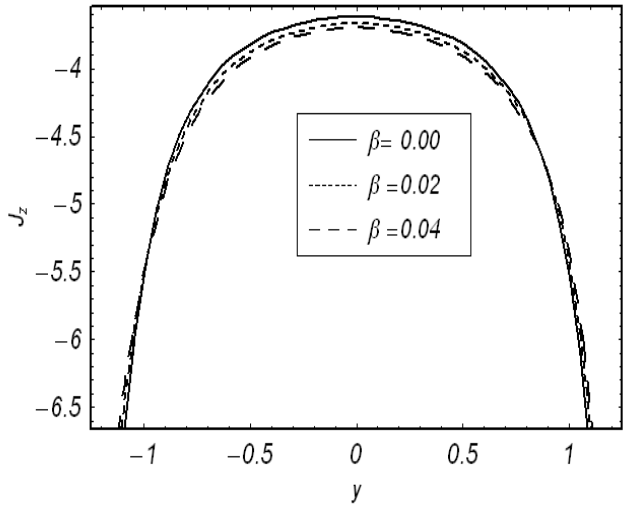

Figure 5b. Current density J_z **versus** y **for** $R_m = 2$, $M = 2.5$, $\alpha = 0.2$, $\xi = 0.02$, $x = 0.2$, $E = 3.5$ **and** $\theta = 2.5$.

magnitude of J_z decreases when M increases at $y = 0$.

Conclusions

This research considered the peristaltic transport of pseudoplastic fluid in the presence of induced magnetic field and wall slip. The important results are summarized as follows:

1. Axial pressure gradient increases with an increase in ξ and decreases with β.
2. Pumping rate increases by increasing M while it decreases with ξ and β.
3. Pressure rise per wavelength is larger in magnitude in case of no-slip condition when compared with slip condition.
3. Axial induced magnetic field increases with increase in magnetic Reynolds number.
4. Current density distribution increases with R_m, ξ, β while it shows opposite behavior for M at $y = 0$.

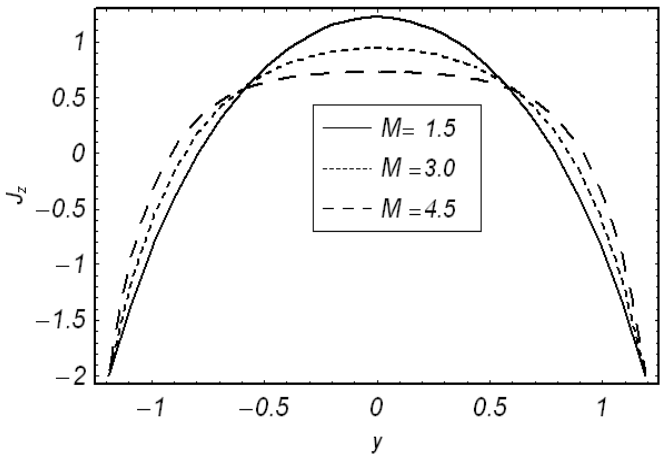

Figure 5c. Current density J_z **versus** y for $M = 1.5$, $\beta = 0.001$, $\alpha = 0.2$, $\xi = 0.001$, $x = 0.2$, $E = 1$ **and** $\theta = 2.5$.

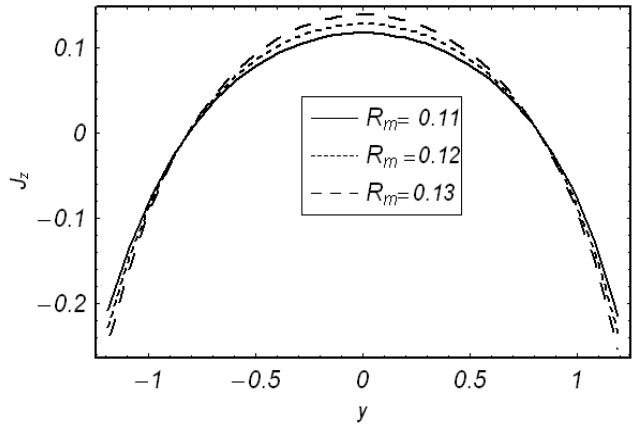

Figure 5b. Current density J_z **versus** y for $M = 1.5$, $\beta = 0.01$, $\alpha = 0.2$, $\xi = 0.01$, $x = 0.2$, $E = 1$ **and** $\theta = 2.5$.

5. Increase in ξ, β and M leads to a decrease in velocity when $y = 0$.

ACKNOWLEDGEMENT

This work was partially supported by Deanship of Scientific Research (DSR), King Abdulaziz University, Jeddah, Saudi Arabia.

REFERENCES

Ali N, Hussain Q, Hayat T, Asghar S (2008). Slip effects on the peristaltic transport of MHD fluid with variable viscosity. Phys. lett. A 372: 1477-1489.

Boger DV (1977). Demonstration of upper and lower Newtonian fluid behavior in a pseudoplastic fluid. Nature. 265: 126-128. .

Ebaid E (2008). Effects of magnetic field and wall slip on the peristaltic transport of a Newtonian fluid in an asymmetric channel. Phys. lett. A 372: 4493-4499.

Elmaboud YA, Mekheimer KS (2011). Non-linear peristaltic transport of a second-order fluid through a porous medium. Appl. Math. Model., 35: 2695-2710.

Haroun MH (2007). Effect of Deborah number and phase difference on peristaltic transport of third order fluid in an asymmetric channel. Comm. NonLinear Sci. Numer. Simul., 12: 1464-1480.

Hayat T, Alvi N, Ali N (2008). Peristaltic mechanism of a Maxwell fluid in an asymmetric channel. Nonlinear Analysis: Real World Applications. 9: 1474-1490.

Hayat T, Hina S (2010). The influence of wall properties on the MHD peristaltic flow of a Maxwell fluid with heat and mass transfer. Nonlinear Analysis: Real World Appl., 11: 3155-3169.

Hayat T, Hina S, Ali N (2010). Simultaneous effects of slip and heat transfer on the peristaltic flow. Comm. Nonlinear Sci. Numer. Simul., 15: 1526-1537.

Hayat T, Hussain Q, Ali N (2008). Influence of partial slip on the peristaltic flow in a porous medium, Phys. Lett. A, 387: 3399-3409. .

Hayat T, Khan Y, Ali N, Mekheimer KS (2010). Effect of an induced magnetic field on the peristaltic flow of a third order fluid. Numer. Methods Partial Diff. Eqs, 26:345-360.

Hayat T, Noreen S (2010). Peristaltic transport of fourth grade fluid with heat transfer and induced magnetic field. C. R Mécanique, 338: 518-528.

Hayat T, Noreen S, Awatif AH (2011). Peristaltic motion of Phan-Thien-Tanner fluid in presence of slip condition. J. Brhe. ((DOI) 10.1007/s12573-011-0033-4).

Hayat T, Qureshi MU, Ali N (2008). The influence of slip on the peristaltic motion of a third order fluid in an asymmetric channel. Phys. Lett. A. 372: 174-178.

Latham TW (1966). Fluid motion in a peristaltic pump. MIT Cambridge MA.

Mekheimer KS (2008). Effect of induced magnetic field on peristaltic flow of a couple stress fluid. Phys. Lett. A. 372: 4271-4278. .

Nadeem S, Akram S (2010). Peristaltic flow of a Williamson fluid in an asymmetric channel. Comm. Nonlinear Sci. Numer. Simul. 15: 1705-1716.

Nadeem S, Akram S (2011). Peristaltic flow of a couple stress fluid under the effect of induced magnetic field in an asymmetric channel. Arch. Appl. Mech. 81: 97-109.

Sapna S (2009). Analysis of non-Newtonian fluid in a stenosed artery. Int. J. Phy. Sci. 4; 663-671.

Shapiro AH, Jaffrin MY, Weinberg SL (1969). Peristaltic pumping with long wavelength at low Reynolds number. J. Fluid Mech. 37: 799-825.

Shehawy EE, Dabe NE, Desoky IE (2006). Slip effects on the peristaltic flow of a non-Newtonian Maxwellian fluid. Acta Mechanica. 186: 141-159.

Shit GC, Roy M, Ng EY (2010). Effect of induced magnetic field on peristaltic flow of a micropolar fluid in an asymmetric channel. Int. J. Numer. Meth. Biomed. Engng. 26: 1380-1403.

Singh J, Rathee R (2010). Analytic solution of two-dimensional model of blood flow with variable viscosity through an indented artery due to LDL effect in the presence of magnetic field. Int. J. Phys. Sci. 12: 1857-1868.

Singh J, Rathee R (2011). Analysis of non-Newtonian blood flow through stenosed vessel in porous medium under the effect of magnetic field. Int. J. Phys. Sci. 6: 2497-2506.

Sobh AM (2008). Interection of couple stresses and slip flow on peristaltic transport in a uniform and non-uniform channel. Turkish J. Eng. Env. Sci. 32: 117-123.

Srinivas S, Gayathri R, Kothandapani M (2009). The influence of slip conditions, wall properties and heat transfer on the MHD peristaltic transport. Comp. Phys. Comm. 180: 2115-2122.

Tripathi D, Pandey SK, Das S (2010). Peristaltic flow of viscoelastic fluid with fractional Maxwell model through a channel. Appl. Math. Comput. 215: 3645-3654.

Tripathi D, Pandey SK, Das D (2011). Peristaltic transport of a generalized Burgers' fluid: Application to the movement of chyme in small intestine. Acta Astronautica. 69: 30-39

Vajravelu K, Sreendah S, Lakshrinarayana P (2011). The influence of heat transfer on peristaltic transport of Jeffrey fluid in a vertical porous stratum, Comm. nonlinear Sci. num. Simul. 16: 3107-3125.

Vishnyakov VI, Pavlov KB (1972). Peristaltic flow of a conductive fluid in a transverse magnetic field. Translated from Magnitnaya Gidrodinamika. 8: 174-178.